FAST MODELING OF A TENSOR INDUCTION TOOL RESPONSE IN A HORIZONTAL WELL IN INHOMOGENEOUS ANISOTROPIC FORMATIONS

Arvidas B. Cheryauka* and Michael S. Zhdanov,
University of Utah, Geology and Geophysics Dept., Salt lake City, UT 84112

ABSTRACT

Induction logs in sub-horizontal wells can provide important information about the properties of the formations. They help to characterize an invasion profile and determine the distances to the oil-water contact and remote beds. However, quantitative interpretation of induction data in a horizontal well, in a general case, requires three-dimensional modeling and analysis. Conventional, axial-coil, induction instruments face significant difficulties to accurately delineate formation and borehole geometry and conductivity anisotropy. In this paper we present a modeling study for a tensor instrument, comprising sets of three mutually orthogonal transmitting and receiving coils. We develop the theoretical solution based on generalized localized approximation. It realizes the 2.5-D algorithmic scheme, which efficiently models the concentric wellbore/invasion structures embedded in layered anisotropic formations. We examine the method's validity using analytical solutions for axially symmetric borehole and invasion models. We also analyze the compatibility of models for horizontal well situations with the models for highly deviated wells. The synthetic results demonstrate a very good match for dipping angles within a range of 90 ± 15 degrees.

INTRODUCTION

The use of horizontal and highly deviated wells has significantly increased the exploration industry's ability to efficiently produce hydrocarbons from the oil and gas bearing formations. In recent years, as the number of horizontal wells has increased, more research has been conducted to understand EM logging tool responses in highly deviated wells (Epov et al., 1996; Anderson et al., 1999; Rabinovich et al., 2000; Ellis and Chiaramonte, 2000). Induction logs in sub-horizontal wells can provide important information about the properties of the formations. However, quantitative interpretation of induction data in a horizontal well, in a general case, requires three-dimensional modeling and analysis. A typical well environment might include an anisotropic layered sequence with an invaded zone. The invasion profile could have a 'drop-like' cross-section due to gravity segregation, where it is not necessarily centered along the borehole axis and may include intrinsic anisotropy. An interpretation model should include all these elements, but conventional, axial-coil, induction instruments experience difficulties in delineating formation and borehole geometry and conductivity anisotropy.

In the present paper we conduct a modeling study for a tensor EM induction instrument composed of mutually orthogonal sets of transmitting and receiving coils. The governing principles and numerical feasibility analysis for this novel induction logging technique have been stated in Bear et al. (1998), Zhdanov et al. (2001), Alumbaugh and Wilt (2001). Here we develop the modeling methods and examine the response abilities of the induction tensor tool prototype in horizontal well models. We develop them for the simulation of synthetic induction data, recorded by the tensor instrument in a 2.5–D dimensional model of an invaded formation in the presence of a layered anisotropic structure. The theoretical response is calculated using a fast algorithm, based on a generalized localized approximation. We consider different formation models, including layered formations with a single horizontal layer and multilayered invaded zones. Our results demonstrate that approximate, but fit-for-purpose, solutions provide a practical tool for fast modeling tensor induction responses in realistic conductivity models.

P

MODELS OF HORIZONTAL WELLS

In this section we briefly summarize the existing knowledge and describe the hypothetical models of induction logging in a horizontal well. These models are usually used in quantitative evaluation of logging in directional wells with horizontal completion.

A typical highly deviated well environment may include an anisotropic layered sequence with a non-symmetrical invaded profile (Pirson, 1983; Ransom, 1995). In fact, the borehole space is a result of rotational drilling in sedimentary rock material which, in most cases, strongly holds a cylindrical shape with a circular cross-section. The tool body is displaced from the borehole axes, since it lies at the bottom of the wellbore. The invasion profile in permeable formations can be formed in two general ways depending on formation material properties. The first typical form of mud penetration is generated in isotropic formation due to gravity segregation. The cross-section of the invasion looks like a drop-like one (Figure 1a). The second type of invasion can happen in formations with a significant ratio of porous permeability in lateral and vertical directions. This difference in permeability is caused by an intrinsic anisotropy or macroanisotropy in a case of thinly-laminated sand-shale sequences. The invaded profile in formations with such anisotropic properties has an elliptical cross-section (Figure 1b). It may have a concentric layered structure as well, since the changes in the borehole mud content often happened due to various stages and regimes of the drilling process. A two-layer structure including invasion zone and annulus is a typical invaded profile in terrain formations as stated in Ransom (1995) and Anderson et al. (1999).

An interpretation model of the real recovered formations should include all these elements. The responses of conventional, axial-coil, induction instruments look quite unfamiliar in these environments. The log diagrams include multiple polarization horns observed at bed boundaries and cannot accurately delineate the invasion characteristics and detailed properties of the formation including anisotropy (Kriegshauser et al., 2000a; Cheryauka et al., 2001b). We suggest that a logging instrument with a tensor observation system is capable of delineating anisotropy parameters, a geometry of invasion, and the properties of the layered structure away from the well (Zhdanov et al., 2001).

THEORETICAL PROBLEM

We begin with a theoretical formulation of an EM boundary value problem to model the tool response in a horizontal well in a layered invaded formation.

We define a coordinate system $\{x', y', z'\}$ with the z'−direction along the tool and borehole lines (Figure 2). The tri-axial transmitter Tx and receiver Rx are located in the z'−axes at the points z'_t and z'_r, respectively. Consider a spatial geometry of the 2-D model of the surrounding medium as a set of concentric cylindrical domains elongated in the z'−direction and embedded into a 1-D planar layered host. For mathematical formulation of the problem, without a loss of generality, we can take into account a single cylindrical region only. We will treat this cylindrical domain of different electric property as an anomalous target of a support V, containing the tool observation system inside. Note that we neglect any anomaly in magnetic property. Let us denote the cylinder's cross-section area as S and its corresponding contour as L with the outer normal $\mathbf{n}$. Define also a vector-radius ρ in the $x'y'$-plane with the origin at the z'-axes. The electromagnetic field depends on time as $e^{-i\omega t}$.

To provide further formulations in a compact form, we will characterize the medium properties by a complex electric conductivity tensor $\sigma(\rho)$,

$$\sigma(\rho) = \gamma(\rho) - i\omega\varepsilon_0\varepsilon(\rho), \tag{1}$$

and a complex magnetic permeability tensor $\mu(\rho)$,

$$\mu(\rho) = i\omega\mu_0(\mathbf{I} + \chi(\rho)), \tag{2}$$

where $\gamma(\rho)$, $\varepsilon(\rho)$, and $\chi(\rho)$ are electric conductivity, relative dielectric constant and magnetic susceptibility tensor functions, respectively. The tensor $\mathbf{I}$ is the identity tensor. The coefficients ε_0 and μ_0 are the dielectric constant and the magnetic permeability of free space.

The total electromagnetic field vectors $\mathbf{E}$, $\mathbf{H}$ at the receiver point can be expressed based on a well-known technique of volume integral equation approach (Weidelt, 1975; Hohmann, 1975):

$$\begin{aligned} \mathbf{E} &= \mathbf{E}_b + \langle \mathbf{G}^{JE}\delta\sigma\mathbf{E}\rangle_V \\ \mathbf{H} &= \mathbf{H}_b + \langle \mathbf{G}^{JH}\delta\sigma\mathbf{E}\rangle_V, \end{aligned} \tag{3}$$

where the inner product notation $\langle \dots \rangle_V$ is used. In formula (3) the lower subscript $'b'$ denotes a background electromagnetic field generated in the media with the background conductivity σ_b and magnetic permeability μ_b. The quantity $\delta\sigma = \sigma - \sigma_b$ is the anomalous conductivity tensor, and $\mathbf{G}^{JE}, \mathbf{G}^{JH}$ are the tensor Green's functions determined in the background model.

The tensor Green's functions of 'electric-to-electric', $\mathbf{G}^{JE}$, and 'electric-to-magnetic', $\mathbf{G}^{JH}$, types satisfy the following second-order differential equations as determined using the same notations in

Cheryauka and Zhdanov (2001c):

$$\begin{aligned}\nabla\times\mu_b^{-1}\nabla\times\mathbf{G}^{JE}-\sigma_b\mathbf{G}^{JE}&=\mathbf{I}\delta(\mathbf{r}-\mathbf{r}_0),\\ \nabla\times\sigma_b^{-1}\nabla\times\mathbf{G}^{JH}-\mu_b\mathbf{G}^{JH}&=\nabla\times\sigma_b^{-1}\mathbf{I}\delta(\mathbf{r}-\mathbf{r}_0),\end{aligned} \quad (4)$$

and they are connected by the first Maxwell's equation,

$$\nabla\times\mathbf{G}^{JH}=\sigma_b\,\mathbf{G}^{JE}+\mathbf{I}\delta(\mathbf{r}-\mathbf{r}_0), \quad (5)$$

where $\mathbf{r}$ and $\mathbf{r}_0$ are radius-vectors of the excitation and measurement points and δ is the Dirac function. Here we assume that the inverse tensor functions σ_b^{-1} and μ_b^{-1} always exist.

Since the medium properties are constant in the z'–direction, we can naturally reduce one dimension applying the one-dimensional spatial transform in this direction. We describe the 1-D spectral Fourier transform by the formulas

$$\begin{aligned}f(\rho,\lambda_z)&=\langle F(\rho,z)e^{-i\lambda_z z'}\rangle_{z'},\\ F(\rho,z')&=\frac{1}{2\pi}\langle f(\rho,\lambda_z)e^{i\lambda_z z'}\rangle_{\lambda}.\end{aligned} \quad (6)$$

In the last formulae λ_z is a horizontal spatial wavenumber, the functions F and f represent any electromagnetic field components, and a small letter denotes a Fourier spectrum of the original function. We can substitute the distance between transmitter and receiver, $z_t'-z_r'$, with the transform argument z', and obtain the spectra of equations (3) as

$$\begin{aligned}\mathbf{e}&=\mathbf{e}_b+\langle\mathbf{g}^{JE}\,\delta\sigma\mathbf{e}\rangle_S\\ \mathbf{h}&=\mathbf{h}_b+\langle\mathbf{g}^{JH}\,\delta\sigma\mathbf{e}\rangle_S.\end{aligned} \quad (7)$$

The system of equations (7) is the system of rigorous Fredholm integral equations of the second kind. Conventional procedures and various approximate methods can be applied for solving this problem. The description of the appropriate solvers, the discussion about their modeling abilities, and the comparative evaluations of the different algorithms can be found, for instance, in our recent papers: Zhdanov et al. (2000); Cheryauka and Zhdanov (2001a).

The mathematical and physical principles of the generalized localized approach have been developed to obtain powerful nonlinear approximations in 3-D inhomogeneous media (Habashy et al., 1993; Zhdanov et. al., 2000). Here we present a slightly different derivation with emphasis on the efficient computation of the nonlinear terms and the discretization of the resultant equations into a class of high-order expansion functions.

According to the key idea of the localized approach, we assume that the dominant contribution to the integral in equation (7) for interior points is produced in a vicinity where the Green's tensor $\mathbf{G}^{JE}$ exhibits a singularity. We introduce a slow varying tensor function α, such that the product $\alpha^{-1}\mathbf{e}$ is also a slow varying function in the interior points of S. We assume, in addition, that this function can depend on location and configuration of the source as well. Performing some simple algebraic manipulations, we obtain an approximate quantity from (7) as

$$\mathbf{e}\approx\mathbf{e}_b+\langle\mathbf{g}^{JE}\delta\sigma\;\alpha\rangle_S\alpha^{-1}\mathbf{e}, \quad (8)$$

or, equivalently,

$$\mathbf{e}\approx\hat{\Lambda}\mathbf{e}_b, \quad (9)$$

where

$$\Lambda^{-1}=\mathbf{I}-\langle\mathbf{g}^{JE}\delta\sigma\alpha\rangle_S\alpha^{-1}. \quad (10)$$

The choice of the function α is based on the idea of simplifing the kernel evaluation in (10) while retaining the accuracy of approximation (9). Under these requirements the kernel can be simplified in some way, or, even, the dimension of the inner product in (10) can be reduced. By choosing a different α, one can construct the different approximations (9). However, the detailed mathematical analysis of this approach lies beyond the framework of the present paper and may constitute the subject of a separate study.

Here we consider the simplest case where the tensor function α is constant and is equal to the identity tensor $\mathbf{I}$. Thus, the tensor Λ becomes a form of the depolarization tensor Γ as it was introduced in a 3-D case by Habashy et al. (1993):

$$\Lambda^{-1}=\Gamma^{-1}=\mathbf{I}-\langle\mathbf{g}^{JE}\delta\sigma\rangle_S, \quad (11)$$

which is source independent and is a function of the medium property distributions only. Assuming that anomalous conductivity tensor $\delta\sigma$ is a constant diagonal tensor within S, we can rewrite (11) as follows:

$$\Lambda^{-1}=\mathbf{I}-\delta\sigma\langle\mathbf{g}^{JE}\rangle_S.$$

Applying equation (5) to the spectra $\mathbf{g}^{JE}$ and $\mathbf{g}^{JH}$, we can rewrite expression (11) as

$$\begin{aligned}\Lambda^{-1}&=\mathbf{I}-\delta\sigma\sigma_b^{-1}\langle\nabla^*\times\mathbf{g}^{JH}-\delta(\rho-\rho_0)\rangle_S\\ &=\sigma_b^{-1}\left[\sigma-\delta\sigma\langle\nabla^*\times\mathbf{g}^{JH}\rangle_S\right],\end{aligned} \quad (12)$$

where operator ∇^* denotes a spectrum of the projection of ∇ in the Fourier transform domain defined by (6).

P

We can use now the Stokes' theorem and transform the surface integral in (12) into the contour integral

$$\sigma_b\Lambda^{-1} = \sigma - \delta\sigma\langle \mathbf{n}\times\mathbf{g}^{JH}\rangle_L. \qquad (13)$$

Here L is the contour surrounding the area S, and $\mathbf{n}$ is the outer normal to L, correspondingly.

The resultant magnetic field at the receiver can be obtained by using formulas (6), (7), (9), and (13):

$$\mathbf{H} = \mathbf{H}_b + \frac{1}{2\pi}\langle \mathbf{h}_a e^{i\lambda_z(z_t'-z_r')}\rangle_\lambda, \qquad (14)$$

where

$$\mathbf{h}_a = \langle \mathbf{g}^{JH}\Lambda\mathbf{j}_b\rangle_S$$
$$\delta\sigma\Lambda^{-1} = \sigma - \delta\sigma\langle \mathbf{n}\times\mathbf{g}^{JH}\rangle_L, \qquad (15)$$

and $\mathbf{j}_b$=$\sigma_b\mathbf{e}_b$ is a spectrum of the electric current in the background medium.

The more complicated models of the invaded profile may include several concentric cylindrical surfaces. This feature will require calculation of the quantities $\mathbf{h}_a$ and Λ as the sums over domains with the constant conductivity $\delta\sigma$. Since all integrals in (14)-(15) are regular, we can easily apply the quadratures based on high order expansion functions.

In the following sections we present the modeling study for the prototype of a tensor induction instrument comprising sets of three mutually orthogonal transmitting and receiving coils. We examine the tool response and compare it with the results obtained by the analytical solution. The models of a circular wellbore and axially symmetric invaded zone are used. The last paragraph of this section deals with the estimation of the influence of the well's deviation at high dipping angles on the tool signals. We consider the differences between the synthetic data calculated in well models using deviated and horizontal trajectories.

MODELING OF WELLBORE

First, we model the induction tool response in the presence of a circular borehole space. Consider a tool composed of point magnetic transmitting and receiving coils with a spacing of 1 m and coil orientations which are parallel to the borehole axis. This hypothetical device has the moment 1 Am^2 and operates at a frequency 20 KHz. The wellbore and outer host formation are characterized by the radius 0.1 m and the resistivity 10 $Ohm-m$, respectively. The resistivity of the wellbore varies in the range [0.1−100] $Ohm-m$. The tool device is centered at the borehole axis.

Figure 3 shows the anomalous magnetic field response calculated by the analytical solution (solid line) and nonlinear approximation algorithm (markers). The tool response in the homogeneous formation without the borehole space is used as a response in the background medium. The in-phase and quadrature signal components are demonstrated at the left and right frames of Figure 3, respectively. The analytic and approximate results have an excellent match within the whole resistivity range.

Comprising a 3-coil induction array with an additional bucking coil is a conventional way to compensate the signal contribution from a borehole space. In Figures 4-5 we numerically examine the response from the 3-coil $MzHz$ and $MxHx$ arrays with the spacings 1/0.75 m and the moments of the 2-coil probes 1/-0.421875 Am^2. The operational frequency and the model parameters of the medium are the same as for the previous experiment (see Figure 3). The total response is normalized by the tool response value in the homogeneous formation. The wellbore compensation for $MzHz$ array can be reached with a relative accuracy of less that 4 % in the whole practical range of the borehole and formation resistivities. The compensation for $MxHx$ works well for in-phase magnetic field component only. For precise compensation of the quadrature component the more detail tool design should be applied.

MODELING OF INVADED ZONE

Next, we extend the model, adding an axially symmetric invaded zone. The goal for the following two numerical tests consists in checking the modeling ability of the nonlinear approximate algorithm, and, second, in analyzing the effect of a broad invasion.

We consider a particular situation with the invasion of the constant resistivity value within the circular cylindrical segment $\rho \in [0.1-1.0]$ m. The background model includes the borehole of resistivity 1 $Ohm-m$, the radius 0.1 m and the outer formation of resistivity 10 $Ohm-m$. The resistivity of the invaded zone is supposed to be varied between the resistivity values of the wellbore and formation. The 2-coil tool prototype, as per the previous experiment described by Figure 3, has the spacing 1 m, the moment 1 Am^2, and operates at 20 KHz. In Figure 6 the matching between the analytic (the solid lines) and approximate (the diamond markers) data is shown for the in-phase and quadrature components of the anomalous magnetic field. One can see that the approximate algorithm still works precisely for the entire resistivity interval of the broad invasion.

The 3-coil $MzHz$ and $MxHx$ induction array configurations and the medium model, chosen above, are used to obtain the results demonstrated in Figures 7-8. The signal is normalized by the signal in the background model with the presence of the borehole. One can see that the compensation of the broad invasion is very limited and exists if the resistivity contrast between invasion and host formation is quite low. If we assume that the invasion resistivity is close to the resistivity of the borehole mud (the left-side abscissa values), the ratios of the tool responses for these 3-coil systems tend to 3.5-4.5 for the corresponding signal components. Thus, the compensation fails for broad conductive invasions, and the signal contribution from the invasion becomes an important subject in well logging studies.

MODELING IN ANISOTROPIC LAYERED FORMATIONS

To describe the spatial orientation of the tool with the tri-axial observation system, we define two Cartesian coordinate systems. The first system $\{x, y, x\}$, the medium coordinate frame, characterizes the vertically transverse isotropic (VTI) model with the $z-$direction, which is perpendicular to the layer's beddings (Figure 9a). We call the distances along the $z-$ and the fixed lateral, say, $x-$ directions as the true vertical depth and the true horizontal distance. The orientations of the tool's transmitting and receiving coils lie along the basic vectors of the primed coordinate system $\{x', y', x'\}$, the instrument coordinate frame, which is different in a well deviated with respect to the perpendicular vector to the layer boundaries (Figure 9b). The γ component of the magnetic field response due to the transmitter dipole oriented in the β direction (the quantities $M_\beta H\gamma$, $\beta, \gamma{=}x', y', z'$) measured at the instrument coordinate system can be expressed in terms of the medium coordinate system using the coordinate transformation with the corresponding rotation matrix (Zhdanov et al., 2001). In this study, we assume that the coordinate transformation is described by dip angle α only, the angle between the $z'-$ and $z-$ axis in the $xz-$plane. Hence, any vector $\mathbf{e}$ in the medium $\{x, y, z\}$ system can be represented through its coordinates given in the instrument $\{x', y', z'\}$ system as

$$\mathbf{e} = \begin{pmatrix} cos\alpha & 0 & sin\alpha \\ 0 & 0 & 0 \\ -sin\alpha & 0 & cos\alpha \end{pmatrix} \mathbf{e}'. \qquad (16)$$

In Figure 10 we consider a generic 3-layer model with a directional well of varying dip angle α. The tool response through the sand reservoir with overlaying shale at the top and gas-oil contact at the bottom is simulated. For simplicity, we use 1-D modeling in the layered formations, ignoring completely the borehole and invasion effects. This formulation is appropriate for geosteering purposes utilizing while-drilling measurements (MWD), where the invasion effect is negligible (Rabinovich et al., 2000). For postdrilling logging with wireline induction tools, the invasion complicates the modeling situation in deviated wells, making it fully 3-D (Kriegshauser et al., 2000b). The 2-D horizontal well model can simplify this problem if the well deviation is close to horizontal, i.e. the dip angle is equal to 90 degrees.

The results of examining the compatibility of horizontal well modeling in highly deviated well paths are shown in Figures 11-12 for the constant trajectories with dip angles of 75 and 85 degrees. We simulate two series of logs with the tensor tool and compare the response for the deviated well (the solid and dotted lines) and the response for the horizontal well (the circle markers) calculated using the Green's tensor library (Cheryauka and Zhdanov, 2001c). The positions of the tool's midbase points coincide for both models. The tool prototype configuration, as it was used before, includes the spacing 1 m, the moment 1 Am^2, and operating frequency 20 kHz. In Figures 11-12 we demonstrate the signals at the co-parallel component configurations $MxHx, MyHy, MzHz$ and combined responses from the cross-component configurations $(MxHz{-}MzHx)/2$. The last quantities show the best match of the results for high values of the dip angle α. One can see that the horizontal well approximation is adequate for replacing with the deviated well model for the dip angle range $[90^0 \pm 15^0]$. The largest differences in the logs occur at the vicinities of 'polarization horns' near the intersections of the interfaces between high-contrast media. However, in real formations there are usually smooth transition zones instead of sharp blocky boundaries. Hence, for practical situations we expect better agreement of the curves when the tool transits the layer beddings.

The well trajectory with a varying dip angle produced by directional drilling can have a complicated

P

but smooth enough form to simulate it with a set of constant dipping intervals. In our next test, we compose the trajectory with five paths of constant deviation of 70, 75, 80, 85, and 90 degrees as shown in Figure 10. We demonstrate the responses of the same tool component configurations in Figure 13. The logs for the in-phase (the dotted line) and quadrature (the solid line) parts of the magnetic field are shown with respect to the true horizontal distance. The modeling curves exhibit the 'horn-like' effects when the well cuts both boundaries.

Analyzing the behavior of the synthetic curves, the appearance of changes in formation properties in the vertical and/or horizontal directions can be predicted. Thus, this knowledge will be very useful while planning wells, on-line tracing of the layer's beds, gas-oil-water contacts, and, otherwise, obtaining the detailed positioning of a well using tensor logging data.

CONCLUSIONS

In this work we have carried out the modeling study on tensor induction logging in subhorizontal wells. The interpretation models of highly deviated and horizontal wells are more complicated in comparison with models of vertical wells and can include a noncentered tool location within the wellbore, nonsymmetric invasion profile, etc. In the deviated well there are significant contributions to the tool response from the surface galvanic charges located at layer boundaries and volume charges due to the presence of formation anisotropy.

We develop the theoretical solution based on a generalized localized approximation, which is able to model concentric wellbore/invasion structures embedded in layered anisotropic formations. We check the validity of the 2.5-D algorithm using the analytical solutions for an axially symmetric borehole and invasion zone. The theoretical data for a horizontal well shows a very good compatibility, utilizing multicomponent observations by tensor logging, with the data computed for a deviated well model with dipping angle of 75 degrees and higher. Our synthetic results demonstrate that approximate but fit-for-purpose solutions can provide a practical tool for fast modeling tensor induction tool responses in realistic 3-D conductivity models.

ACKNOWLEDGMENTS

The authors acknowledge the support of the University of Utah Consortium for Electromagnetic Modeling and Inversion (CEMI), which includes AGIP, Baker Atlas Logging Services, BHP Minerals, ExxonMobil Upstream Research Company, INCO Exploration, International Energy Services, Japan National Oil Corporation, MINDECO, Naval Research Laboratory, Rio Tinto-Kennecott, Sumitomo Metal Mining Co., and 3JTech Corporation.

The authors would like to thank Prof. Michael Epov, Institute for Geophysics, Novosibirsk and Dr. Berthold Kriegshauser, Baker Atlas Logging Services for their constructive suggestions during this work.

REFERENCES

Alumbaugh, D. L., and M. J. Wilt, 2001, A numerical feasibility study of three dimensional imaging from a single borehole: Petrophysics, **42**, No. 1, 19-31.

Anderson, B., Barber, T., Druskin, V., Lee, P., Dussan, E., Knizhnerman, L., and S. Davydycheva, 1999, The response of multiarray induction tools in highly dipping formations with invasion and in arbitrary 3D geometry: The Log Analyst, **40**, No.5, 327-344.

Bear, D. R., van der Horst, M., Strack, K.-M., and L. A. Tabarovsky, 1998, Electrical logging of a laminated formation: International Patent WO 98/00733.

Cheryauka, A. B., and M. S. Zhdanov, 2001a, Nonlinear approximations for an EM scattering problem in a medium with joint electrical and magnetic inhomogeneities: submitted in Radio Science.

Cheryauka, A. B., Zhdanov, M. S., and M. Sato, 2001b, Induction Logging with Directional Coil Polarizations: Modeling and Resolution Analysis: Petrophysics (in press).

Cheryauka, A. B., and M. S. Zhdanov, 2001c, Electromagnetic tensor Green's functions in transversely isotropic layered media: IEEE Trans. on Geosc. and Rem. Sens., in submission.

Ellis, D., V., and J. M. Chiaramonte, 2000, Interpreting neutron logs in horizontal wells: a forward modeling: Petrophysics, **41**, No. 1, 23-32.

Epov, M. I., Cheryauka, A. B., and M. N. Nikitenko, 1996, High-frequency electromagnetic soundings in deviated boreholes with horizontal completion: Proc. of 58^{th} Conf. of EAGE Annual Meeting, Amsterdam, P170.

Habashy, T. M., Groom, R. W., and B. R. Spies, 1993, Beyond the Born and Rytov approximations: a nonlinear approach to electromagnetic scattering: Journal of Geophysical Research, **98**, B2, 1759-1775.

Hohmann, G. W., 1975, Three-dimensional induced polarization and electromagnetic modeling: Geophysics, **40**, 309-324.

Kriegshauser, B. F., Fanini, O. N., Forgang, S., Mollison, R. A., Yu, L., Gupta, P. K., Koelman, J. M. V., and J. van Popta, 2000a, Increased Oil-In-Place in low-resistivity reservoirs from multicomponent induction log data: Proc. of SPWLA 41^{st} Annual Logging Symposium, paper C.

Kriegshauser, B. F., Fanini, O. N., Yu, L., and P. K. Gupta, 2000b, Advanced inversion techniques for multicomponent induction log data: Proc. of SEG 69^{th} Annual Meeting, Calgary, paper D.

Pirson, S. J. 1983, Geological Well Log Analysis: Gulf Publishing Comp., Houston.

Rabinovich, M., Frenkel M., Geldmacher, I. M., Georgi D., Mezzatesta, A., Tabarovsky, L., Wang, T., Fidan, M., and D. MacCallum, 2000, Application of array resistivity measurements in horizontal wells: The Leading Edge, **19**, No. 4, 413-422.

Ransom, R.,C., 1995, Practical formation evaluation: John Wiley & Sons, Inc.

Weidelt, P., 1975, Electromagnetic induction in three-dimensional structures: Geophysics, **41**, 85-109.

Zhdanov, M. S., Dmitriev, V.I., Fang, S., and G. Hursan, 2000, Quasi-analytical approximations and series in electromagnetic modeling: Geophysics, **65**, No. 6, 1746-1757.

Zhdanov, M. S., Peksen, E., and D. Kennedy, 2001, Foundations of tensor induction well logging: Petrophysics (in press).

ABOUT THE AUTHORS

Arvidas Cheryauka received his M.Sc. in Geophysics from the Novosibirsk State University, Russia in 1986 and a Ph.D in Geophysics from Institute for Geophysics, Siberian Branch of Russian Academy of Sciences in 1989. From 1995-1998 he worked as a consultant for LOOCH Geophysical Engineering and Baker Atlas companies. During 1998-1999, Arvidas was a visiting scientist with Tohoku University in Sendai, Japan. Since 1999 he has been working as a research scientist with Consortium for Electromagnetic Modeling and Inversion, University of Utah on the development of new array technologies for subsurface and well-logging sensing.

Michael Zhdanov joined the University of Utah as a full professor in 1993. He has been Director of the Consortium for Electromagnetic Inversion and Modeling since 1995. He received a Ph.D. in 1970 from Moscow State University. He spent more than twenty years as a professor at the Moscow Academy of Oil and Gas, and as the head of the Department of Deep Electromagnetic Study and as Deputy Director of the Geoelectromagnetic Research Institute of the United Institute of Physics of the Earth, Russian Academy of Sciences, Moscow, before moving to the University of Utah. In 1990 he was awarded an Honorary Diploma of Gauss Professorship by Gottingen Academy of Sciences, Germany. In 1991 he was elected Full Member of the Russian Academy of Natural Sciences. He became Honorary Professor of the China National Center of Geological Exploration Technology in 1997.

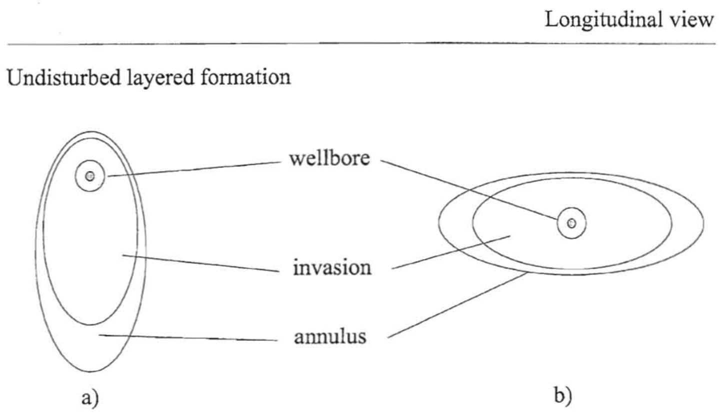

Figure 1: The structural elements of a horizontal well model are the tool body space, the wellbore, the invasion profile, and layered anisotropic formation. The models of invaded profiles: the "drop-like" invaded zone due to gravity segregation (a) and the elliptical invaded zone in a permeable anisotropic formation (b). The invaded zone can include several cylindrical layers as a result of changes in the drilling regime. The two-layer structure (invasion and annulus) is a typical invaded profile in terrain formations (Ransom, 1995).

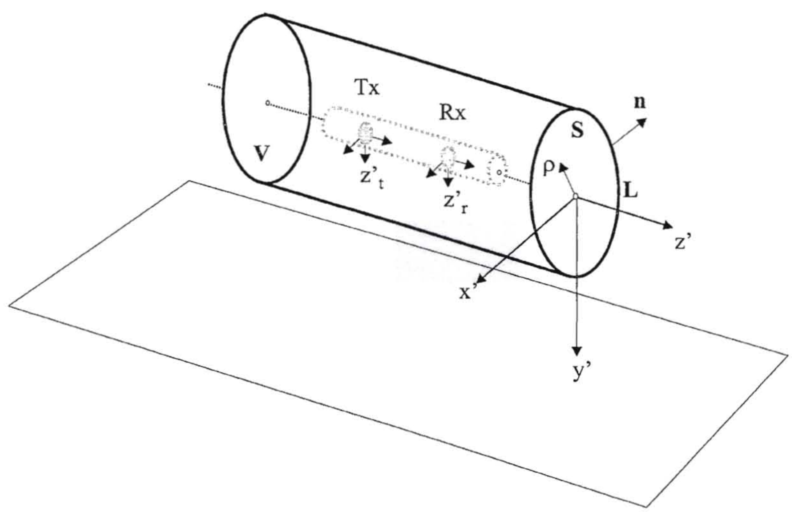

Figure 2: The mathematical model of a horizontal well. A 2-D model's geometry can consist of a set of cylindrical and planar interfaces extended along the $z'-$ direction. The shape of the cylindrical body is described by volume V, cross-section area S and contour of cross-section L. Vector ρ is defined at the $x'y'-$plane. The tri-axial induction transmitter Tx and receiver Rx are located on the z'-axis at points z'_t and z'_r, respectively.

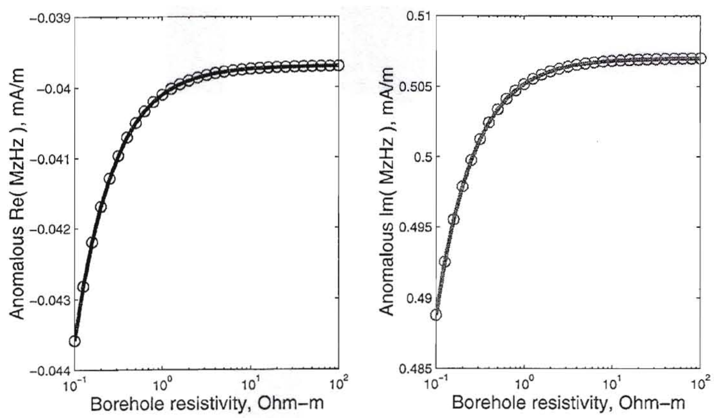

Figure 3: The modeling of a borehole: the comparison between the anomalous magnetic fields calculated by the analytic solution (the solid lines) and nonlinear approximation (the circles).

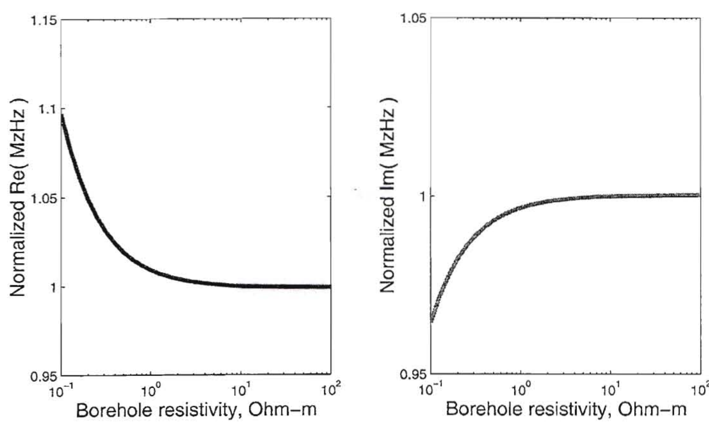

Figure 4: Borehole compensation with the 3-coil $MzHz$ induction tool.

P

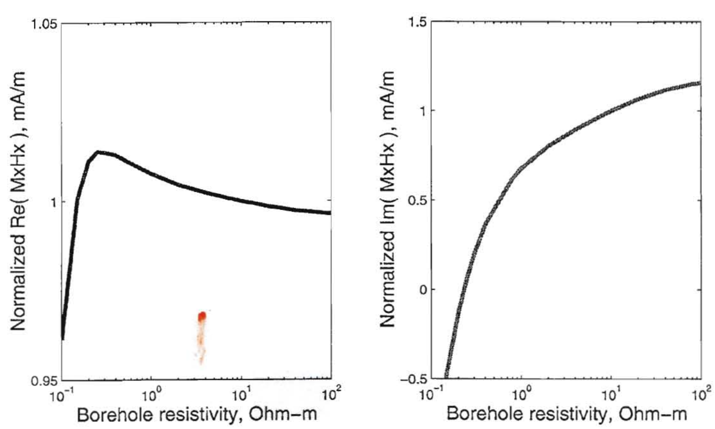

Figure 5: Borehole compensation with the 3-coil $MxHx$ induction tool.

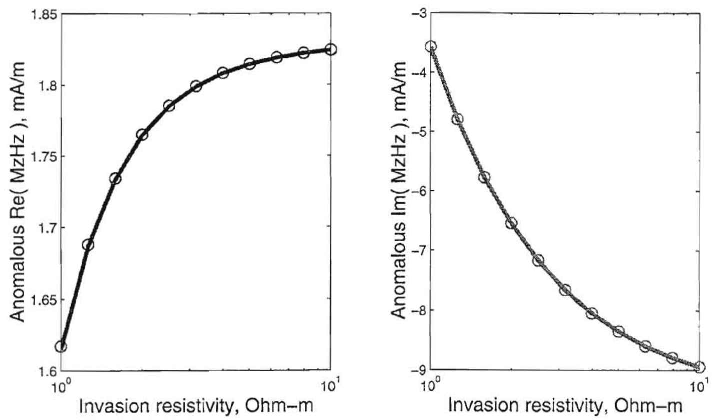

Figure 6: The modeling of an invaded zone: the comparison between the anomalous magnetic fields calcu lated by the analytic solution (the solid lines) and nonlinear approximation (the circles).

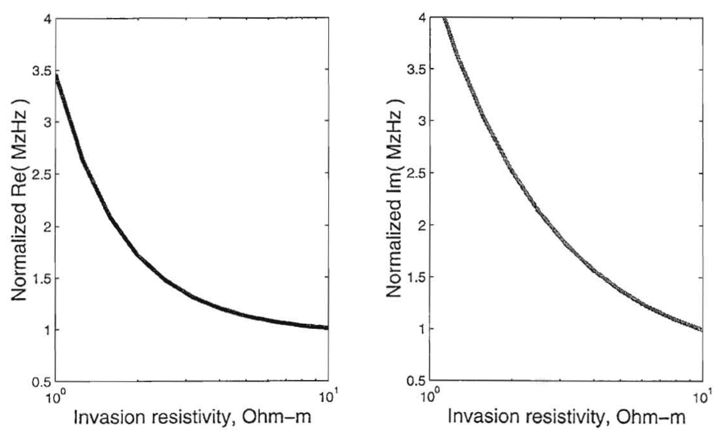

Figure 7: The invaded zone compensation by the 3-coil $MzHz$ induction tool.

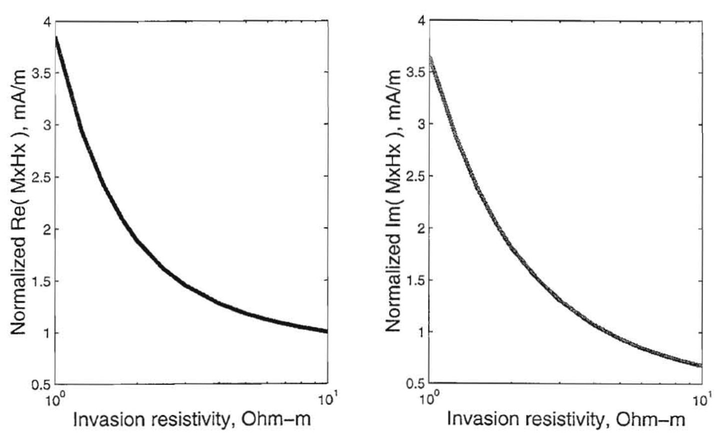

Figure 8: The invaded zone compensation by the 3-coil $MxHx$ induction tool.

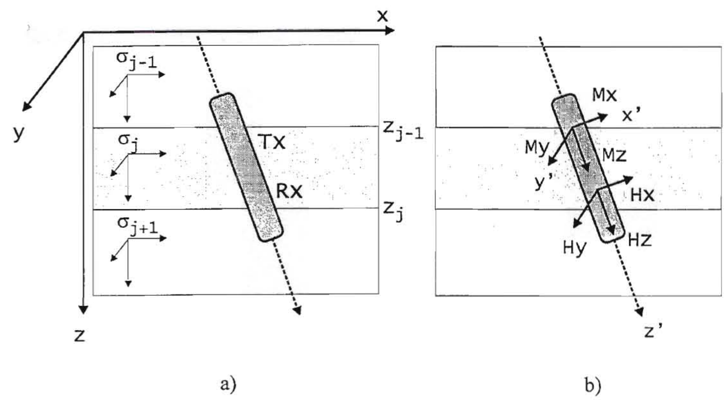

Figure 9: The tensor induction tool in a layered anisotropic formation: the model coordinate system $\{x, y, z\}$ (a) and the instrument coordinate system $\{x', y', z'\}$.

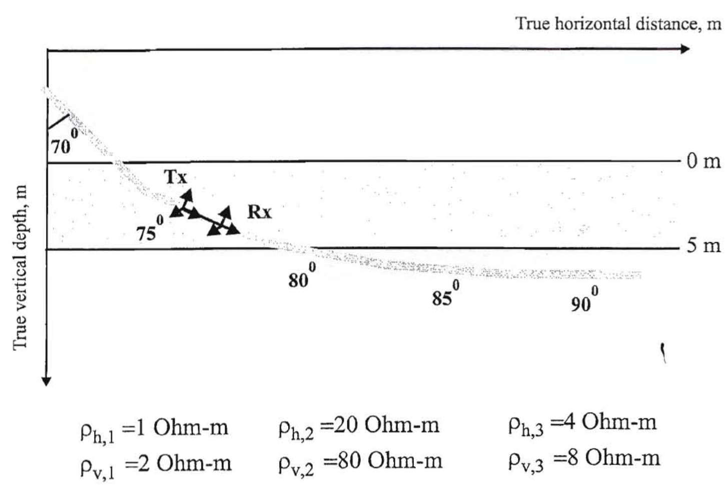

Figure 10: The model of the 3-layer anisotropic formation and directional well of varying dipping angle.

P

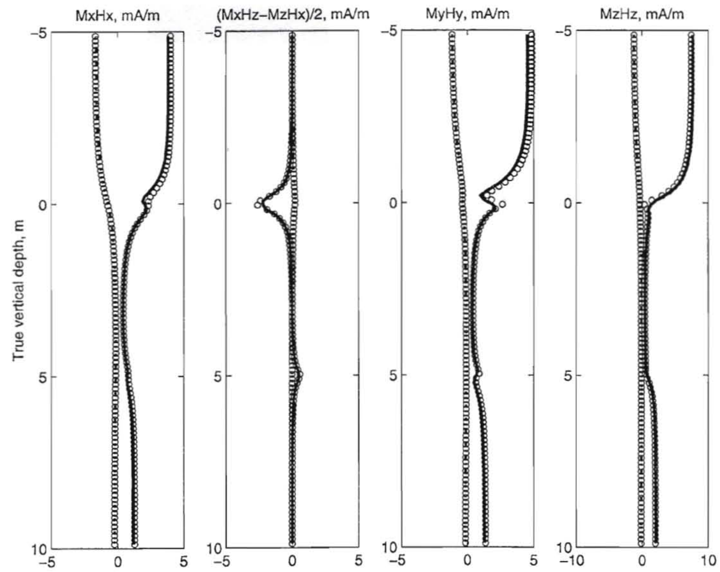

Figure 11: The tensor logs in the 3-layer anisotropic model and deviated well of 75°. The two parts of the magnetic field (the in-phase and quadrature components) are calculated by using the code for a deviated well (the dotted and solid lines) and the code for a horizontal well (the circles).

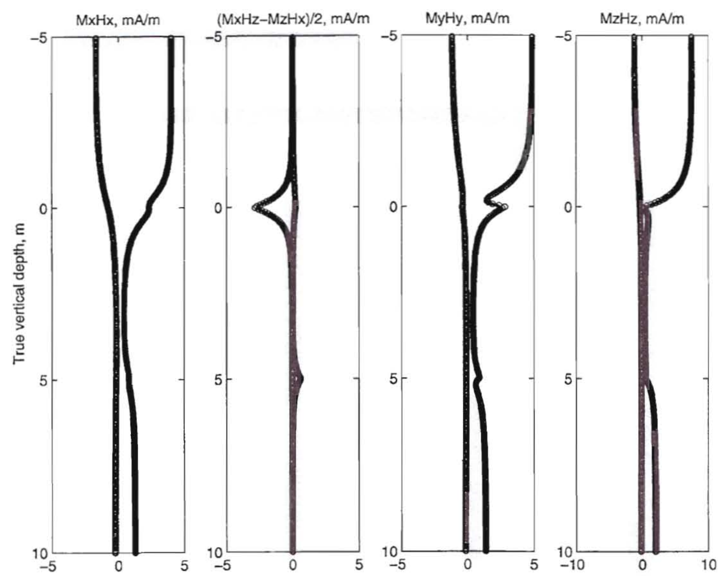

Figure 12: The tensor logs in the 3-layer anisotropic model and deviated well of 85°. The two parts of the magnetic field (the in-phase and quadrature components) are calculated by using the code for a deviated well (the dotted and solid lines) and the code for a horizontal well (the circles).

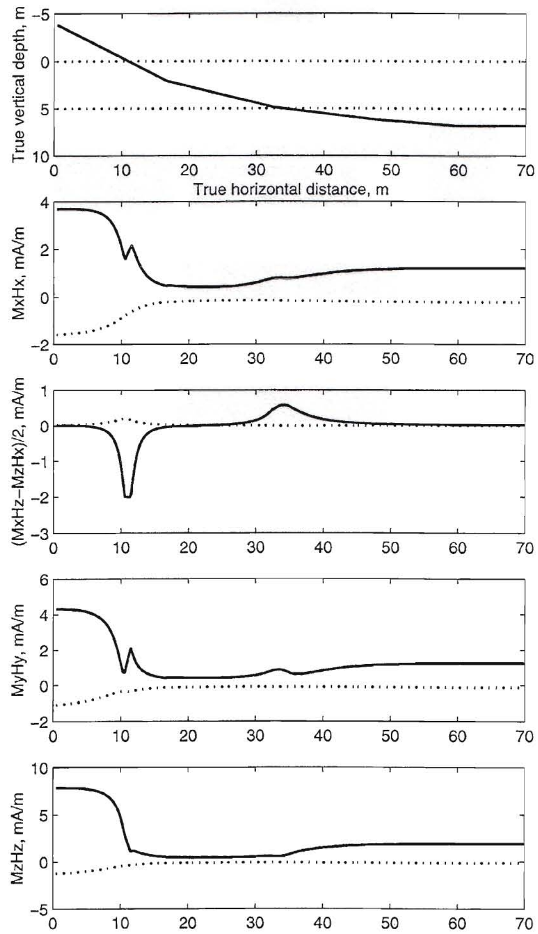

Figure 13: The tensor logs in the subhorizontal well with varying dipping angles. The top frame shows the trajectory and the locations of the formation boundaries. The four frames below demonstrate the tool responses for the tool component configurations $MxHx, (MxHz - MzHx)/2, MyHy$, and $MzHz$. The in-phase and quadrature parts of the magnetic field are shown by the dashed and solid lines, respectively. The magnetic field in air is subtracted from the total signals.

P